



HAL
open science

How Reproducible Are Surface Areas Calculated from the BET Equation?

Johannes Osterrieth, James Rampersad, David Madden, Nakul Rampal, Luka Skoric, Bethany Connolly, Mark Allendorf, Vitalie Stavila, Jonathan Snider, Rob Ameloot, et al.

► **To cite this version:**

Johannes Osterrieth, James Rampersad, David Madden, Nakul Rampal, Luka Skoric, et al.. How Reproducible Are Surface Areas Calculated from the BET Equation?. 2021. hal-03453291

HAL Id: hal-03453291

<https://hal.science/hal-03453291>

Preprint submitted on 28 Nov 2021

HAL is a multi-disciplinary open access archive for the deposit and dissemination of scientific research documents, whether they are published or not. The documents may come from teaching and research institutions in France or abroad, or from public or private research centers.

L'archive ouverte pluridisciplinaire **HAL**, est destinée au dépôt et à la diffusion de documents scientifiques de niveau recherche, publiés ou non, émanant des établissements d'enseignement et de recherche français ou étrangers, des laboratoires publics ou privés.

1 How reproducible are surface areas calculated from the BET 2 equation?

3 Johannes W. M. Osterrieth^a, James Rampersad^a, David Madden^a, Nakul Rampal^a, Luka Skoric^b,
4 Bethany Connolly^a; Mark D. Allendorf^c, Vitalie Stavila^c, Jonathan L. Snider^c; Rob Ameloot^d, João
5 Marreiros^d; Conchi Ania^e; Diana Azevedo^f, Enrique Vilarrasa-Garcia^f, Bianca F. Santos^f; Xian-He
6 Bu^g, Xe Zang^g; Hana Bunzer^h; Neil R. Champnessⁱ, Sarah L. Griffinⁱ; Banglin Chen^j, Rui-Biao Lin^j;
7 Benoit Coasne^k; Seth Cohen^l, Jessica C. Moreton^l; Yamil J. Colon^m; Linjiang Chenⁿ, Rob Clowesⁿ;
8 François-Xavier Coudert^o; Yong Cu^p, Bang Hou^p; Deanna M. D'Alessandro^q, Patrick W. Doheny^q;
9 Mircea Dincă^r, Chenyue Sun^r; Christian Doonan^s, Michael Thomas Huxley^s; Jack D. Evans^t; Paolo
10 Falcaro^u, Raffaele Ricco^u; Omar Farha^v, Karam B. Idrees^v, Timur Islamoglu^v; Pingyun Feng^w,
11 Huajun Yang^w; Ross S. Forgan^x, Dominic Bara^x; Shuhei Furukawa^y, Eli Sanchez^y; Jorge Gascon^z,
12 Selvedin Telalovic^z; Sujit K. Ghosh^{aa}, Soumya Mukherjee^{aa}; Matthew R. Hill^{ab}, Muhammad Munir
13 Sadiq^{ab}; Patricia Horcajada^{ac}, Pablo Salcedo-Abraira^{ac}; Katsumi Kaneko^{ad}, Radovan Kukobat^{ad};
14 Jeff Kevin^{ae}; Seda Keskin^{af}; Susumu Kitagawa^{ag}, Kenichi Otake^{ag}; Ryan P. Lively^{ah}, Stephen J. A.
15 DeWitt^{ah}; Phillip Llewellyn^{aj}; Bettina V. Lotsch^{aj,ak}, Sebastian T. Emmerling^{aj,ak}, Alexander M.
16 Pütz^{aj,ak}; Carlos Martí-Gastaldo^{al}, Natalia M. Padia^{al}; Javier García-Martínez^{am}, Noemi Linares^{am};
17 Daniel MasPOCH^{an,ao}, Jose A. Suárez del Pino^{ao}; Peyman Moghadam^{ap}, Rama Oktavian^{ap}; Russel
18 E. Morris^{aq}, Paul S. Wheatley^{aq}; Jorge Navarro^{ar}; Camille Petit^{as}, David Danac^{as}; Matthew J.
19 Rosseinsky^{at}, Alexandros P. Katsoulidis^{at}; Martin Schröder^{au}, Xue Han^{au}, Sihai Yang^{au}; Christian
20 Serre^{av}, Georges Mouchaham^{av}; David S. Sholl^{ah}, Raghuram Thyagarajan^{ah}; Daniel Siderius^{u,φ,aw};
21 Randall Q. Snurr^{ax}, Rebecca B. Goncalves^{ay}; Shane G. Telfer^{az}, Seok J. Lee^{az}; Valeska P. Tin^{ba},
22 Jemma L. Rowlandson^{ba}; Takashi Uemura^{bb}, Tomoya Iiyuka^{bb}; Monique A. van der Veen^{bc}, Davide
23 Rega^{bc}; Veronique Van Speybroeck^{bd}, Sven M. J. Rogge^{bd}, Aran Lammaire^{bd}; Krista S. Walton^{ah},
24 Lukas W. Bingel^{ah}; Stefan Wuttke^{be,bf}, Jacopo Andreo^{be,bf}; Omar Yaghi^{bg,bh}, Bing Zhang^{bg}; Cafer T.
25 Yavuz^{bi}, Thien S. Nguyen^{bi}; Felix Zamora^{bj}, Carmen Montoro^{bj}; Hongcai Zhou^{bk}, Angelo Kirchon^{bk};
26 and David Fairen-Jimenez^{a,*}

27

28 ^a Adsorption & Advanced Materials Laboratory (A²ML), Department of Chemical Engineering & Biotechnology,
29 University of Cambridge, Philippa Fawcett Drive, Cambridge CB3 0AS, UK

30 ^b Cavendish Laboratory, University of Cambridge, JJ Thomson Avenue, CB3 0HE, Cambridge, United
31 Kingdom

32 ^c Sandia National Laboratories, 7011 East Avenue, Livermore, California 94550, United States

33 ^d cMACS, Department of Microbial and Molecular Systems (M²S), KU Leuven, 3001 Leuven, Belgium

34 ^e CEMHTI, CNRS (UPR 3079), Université d'Orléans, 45071 Orléans, France

35 ^f LPACO2/GPSA, Department of Chemical Engineering, Federal University of Ceará, 60455-760 Fortaleza
36 (CE), Brazil

37 ^g School of Materials Science and Engineering, National Institute for Advanced Materials, Nankai University,
38 Tianjin 300350, China

39 ^h Chair of Solid State and Materials Chemistry, Institute of Physics, University of Augsburg,
40 Universitaetsstrasse 1, Augsburg 86159, Germany

41 ⁱ School of Chemistry, University of Nottingham, University Park, Nottingham, NG7 2RD UK

42 ^j Department of Chemistry, University of Texas at San Antonio, One UTSA Circle, San Antonio, TX 78249-
43 0698, USA

44 ^k Univ. Grenoble Alpes, CNRS, LIPhy, 38000 Grenoble, France

45 ^l Department of Chemistry and Biochemistry, University of California, San Diego, La Jolla, California, 92093
46 USA

47 ^m Department of Chemical and Biomolecular Engineering, University of Notre Dame, Notre Dame, IN, 46556,
48 USA

49 ⁿ Leverhulme Research Centre for Functional Materials Design, Materials Innovation Factory and Department
50 of Chemistry, University of Liverpool, Liverpool, UK

51 ^o Chimie ParisTech, PSL University, CNRS, Institut de Recherche de Chimie Paris, 75005 Paris, France

52 ^p School of Chemistry and Chemical Engineering, Shanghai Jiaotong University, 800 Dongchuan Road,
53 Minhang District, Shanghai

54 ^q School of Chemistry, The University of Sydney, New South Wales, 2006, Australia

55 ^r Department of Chemistry, Massachusetts Institute of Technology, Cambridge, Massachusetts 02139, USA

56 ^s Centre for Advanced Nanomaterials and Department of Chemistry, The University of Adelaide, North Terrace,
57 Adelaide, SA 5000, Australia

58 ^t Department of Inorganic Chemistry, Technische Universität Dresden, Bergstrasse 66, 01062, Dresden,
59 Germany

60 ^u Institute of Physical and Theoretical Chemistry, Graz University of Technology, Graz, Austria

61 ^v Department of Chemistry and International Institute of Nanotechnology, Northwestern University, 2145
62 Sheridan Road, Evanston, Illinois 60208, United States

63 ^w Department of Chemistry, University of California, Riverside, California 92521, USA

64 ^x WestCHEM School of Chemistry, University of Glasgow, Glasgow, UK

65 ^y Institute for Integrated Cell-Material Sciences, Kyoto University, Yoshida, Sakyo-ku, Kyoto 606-8501, Japan

66 ^z KAUST Catalysis Center (KCC), King Abdullah University of Science and Technology, P.O.Box 4700, 23955-
67 6900, Thuwal-Jeddah, Kingdom of Saudi Arabia

68 ^{aa} Department of Chemistry, Indian Institute of Science Education and Research (IISER), Pune, Dr. Homi
69 Bhabha Road, Pashan, Pune 411008, India

70 ^{ab} CSIRO, Private Bag 33, Clayton South MDC, VIC 3169, Australia and Department of Chemical Engineering,
71 Monash University, Clayton, VIC 3168, Australia

72 ^{ac} Advanced Porous Materials Unit (APMU), IMDEA Energy, Avda. Ramón de la Sagra 3, E-28935 Móstoles,
73 Madrid, Spain

74 ^{ad} Research Initiative for Supra-Materials, Shinshu University, Nagano, Japan

75 ^{ae} Micromeritics Instrument Corporation, Norcross, GA 30093, USA

76 ^{af} Department of Chemical and Biological Engineering, Koc University, Rumelifeneri Yolu 34450 Sariyer,
77 Istanbul, Turkey

78 ^{ag} Institute for Integrated Cell-Material Sciences (WPI-iCeMS), Kyoto University Institute for Advanced Study
79 (KUIAS), Kyoto University, Yoshida Ushinomiya-cho, Sakyo-ku, Kyoto 606-8501, Japan

80 ^{ah} School of Chemical & Biomolecular Engineering, Georgia Institute of Technology, Atlanta, GA 30332, USA

81 ^{ai} CNRS / Aix-Marseille Univ. / TOTAL
82 ^{aj} Max Planck Institute for Solid State Research, Heisenbergstrasse 1, 70569 Stuttgart, Germany
83 ^{ak} Department of Chemistry, University of Munich (LMU), Butenandtstrasse 5-13, 81377 Munich, Germany
84 ^{al} Instituto de Ciencia Molecular (ICMol), Universitat de València, Paterna 46980, València, Spain
85 ^{am} Laboratorio de Nanotecnología Molecular, Departamento de Química Inorgánica, Universidad de Alicante,
86 Ctra. San Vicente-Alicante s/n, E-03690 San Vicente del Raspeig, Spain
87 ^{an} ICREA, Pg. Lluís Companys 23, Barcelona, 08010, Spain
88 ^{ao} Catalan Institute of Nanoscience and Nanotechnology (ICN2), CSIC and the Barcelona Institute of Science
89 and Technology. Campus UAB, Bellaterra, 08193 Barcelona, Spain
90 ^{ap} Department of Chemical and Biological Engineering, University of Sheffield, Sheffield S1 3JD, UK
91 ^{aq} School of Chemistry, University of St Andrews, North Haugh, St Andrews, KY16 9ST, UK
92 ^{ar} Departamento de Química Inorgánica, Universidad de Granada, 18071 Granada, Spain
93 ^{as} Barrer Centre, Department of Chemical Engineering, Imperial College London, London, U.K., SW7 2AZ
94 ^{at} Materials Innovation Factory, Department of Chemistry, University of Liverpool, Liverpool, L7 3NY, UK
95 ^{au} School of Chemistry, The University of Manchester, Manchester, U.K. M13 9PL
96 ^{av} Institut des Matériaux Poreux de Paris, Ecole Normale Supérieure, ESPCI Paris, CNRS, PSL University,
97 75005 Paris, France
98 ^{aw} Chemical Sciences Division, National Institute of Standards and Technology, Gaithersburg, Maryland USA
99 20899-8320
100 ^{ax} Departments of Chemical & Biological Engineering, Northwestern University, 2145 Sheridan Road,
101 Evanston, Illinois 60208, USA
102 ^{ay} Department of Chemistry, Northwestern University, 2145 Sheridan Road, Evanston, Illinois 60208, USA
103 ^{az} MacDiarmid Institute of Advanced Materials and Nanotechnology, School of Fundamental Sciences, Massey
104 University, Palmerston North, New Zealand
105 ^{ba} Department of Mechanical Engineering, University of Bristol, Bristol BS8 1TR, U.K.
106 ^{bb} Department of Advanced Materials Science, Graduate School of Frontier Sciences, The University of Tokyo,
107 5-1-5 Kashiwanoha, Kashiwa, Chiba 277-8561, Japan
108 ^{bc} Department of Chemical Engineering, Delft University of Technology, van der Maasweg 9, 2629HZ Delft,
109 the Netherlands
110 ^{bd} Center for Molecular Modeling (CMM), Ghent University, Technologiepark 46, B-9052 Zwijnaarde, Belgium
111 ^{be} BCMaterials, Basque Center for Materials, Applications and Nanostructures, UPV/EHU Science Park,
112 48940, Leioa, Spain
113 ^{bf} IKERBASQUE, Basque Foundation for Science, 48009, Bilbao, Spain
114 ^{bg} Department of Chemistry, University of California—Berkeley; Kavli Energy Nanoscience Institute at UC
115 Berkeley
116 ^{bh} Berkeley Global Science Institute, Berkeley, California 94720, United States
117 ^{bi} Department of Chemical and Biomolecular Engineering, Korea Advanced Institute of Science and
118 Technology (KAIST), Yuseong-gu, 34141 Daejeon, Korea
119 ^{bj} Departamento de Química Inorgánica, Universidad Autónoma de Madrid, 28049 Madrid, Spain
120 ^{bk} Chemistry Department -Texas A&M University
121 ^ψ Official contribution of the National Institute of Standards and Technology (NIST), not subject to copyright in
122 the United States of America

123 ^φ Certain commercially available items may be identified in this paper. This identification does not imply
124 recommendation by NIST, nor does it imply that it is the best available for the purposes described

125 * E-mail: df334@cam.ac.uk

126

127

128 **To the editor:**

129 The Brunauer-Emmett-Teller (BET) equation is arguably one of the most used equations in physical
130 chemistry and porosimetry. Since its conception in the 1930s¹ to estimate open surfaces whilst
131 working with adsorbents of the time such as Fe/Cu catalysts, silica gel, and charcoal, it has found
132 widespread use in the characterisation of synthetic zeolites.² Furthermore, it gained considerable
133 momentum following the discovery of more complex porous materials such as mesoporous silicas,³
134 porous coordination polymers (PCPs),⁴ metal-organic frameworks (MOFs),⁵ and covalent organic
135 frameworks (COFs).⁶ Novel porous materials are of significant academic and industrial interest due
136 to their applications in gas storage and separation,^{7–10} catalysis,¹¹ and drug delivery,¹² and the BET
137 area is their *de facto* standard for the characterisation. It has been recognized by the International
138 Union of Pure and Applied Chemistry (IUPAC) as “the most widely used procedure for evaluating
139 the surface area of porous and finely-divided materials”,^{13,14} and it has been an International
140 Organization for Standardization (ISO) standard for surface area determination since 1995.¹⁵ Whilst
141 concerns over the applicability of the BET theory for microporous materials are important, it remains,
142 arguably, the most important figure of merit for porous materials. Given the broad use of the BET
143 equation, it is not surprising to see that much has been written on the *applicability* and the *accuracy*
144 of the BET theory – that is, its model of the adsorption process – and on the reproducibility of the
145 raw data, *i.e.* the adsorption isotherm.^{16–20}

146 The advent of materials with more complex pore networks and dynamic frameworks through
147 material design strategies such as reticular chemistry has boosted interest in BET theory (**Figure**
148 **S1**) and given rise to reported BET areas in excess of 8,000 m² g⁻¹.^{8,21,22} Often, these modern
149 materials have complex adsorption isotherms that are more problematic or ambiguous to fit to the
150 BET model, *e.g.* several steps can occur due to different pore types and/or flexibility being present
151 in the material.²³ Whilst adsorption rigs capable of ultra-low pressure (<10⁻⁵ mbar) recordings have
152 been developed, reliance on manual calculations of BET areas remains commonplace. In this
153 context, ‘manual’ refers to the judicious selection of the *optimal pressure range* by a scientist, be it
154 through a self-developed spreadsheet or commercial software. This raises the question of the
155 *reproducibility* of BET calculations *from the same measured isotherm* but from different assessors.

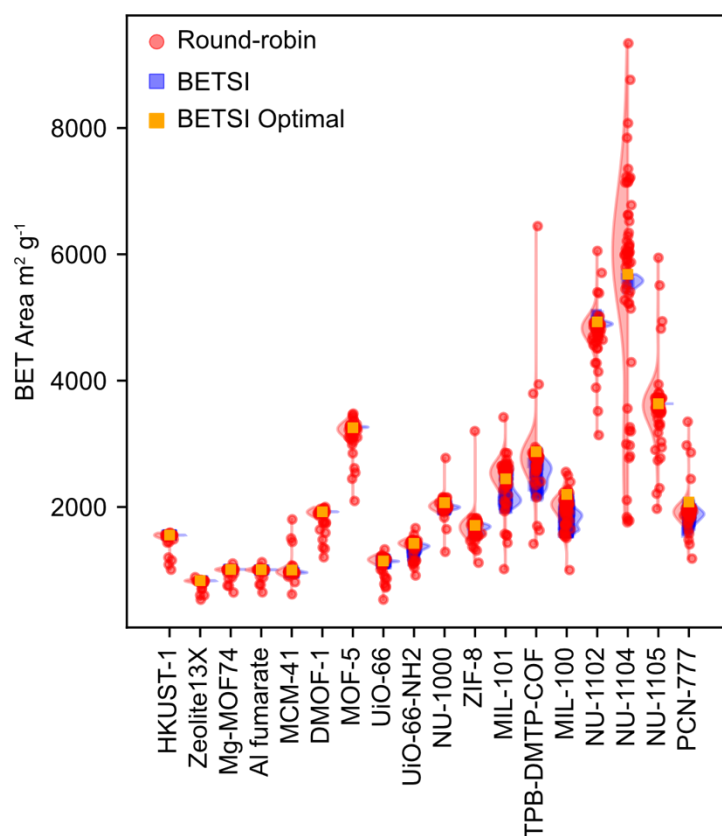
156 The eponymously named Rouquerol criteria (**Section S2**, Supplementary Information) aim to
157 ensure good practice in identifying a valid fitting range, and, as such, they have found widespread
158 acceptance in the literature and have been adopted in both IUPAC and ISO standards.^{13–15,17,18,24,25}
159 Despite this safeguard, we herein propose that current BET area calculations are many times
160 irreproducible for two reasons: first, the Rouquerol criteria are indeterminate in identifying the correct

161 fitting region, as they apply to multiple regions simultaneously. Second, even if they were
162 determinate, they are too cumbersome and lengthy to be systematically implemented and are
163 therefore often neglected in practice.

164 To prove our hypothesis and to assess the current spread of BET calculation results, we have
165 shared a set of 18 experimental isotherms representing four classes of porous materials (zeolites,
166 mesoporous silicas, MOFs, and COFs) with 60 laboratories with expertise in adsorption science and
167 synthesis of porous materials. In this round-robin exercise, we asked the researchers to calculate
168 the BET areas in the way they saw most fit. More details about the specific materials and the
169 adsorption isotherms, sampled both from our laboratory and from the NIST/ARPA-E database,²⁶ are
170 included in the Supplementary Information, **Section S12**. To avoid any recognition bias, all
171 isotherms were anonymised and scaled off arbitrarily.

172 In parallel, we have developed a computational approach to calculating BET areas that only
173 requires the adsorption isotherm as input data. The BET Surface Identification (BETSI) algorithm,
174 steps through *all* possible fitting regions and outputs a full distribution of BET areas that are
175 consistent under the Rouquerol criteria. We further propose an addition to the criteria that makes,
176 for the first time, an unambiguous assignment of BET areas from an adsorption isotherm possible:
177 the ideal fitting range ends on the highest permissible pressure point under all criteria, representing
178 the end of the bulk adsorptive activity of the material, *i.e.* the isotherm knee. Further, it is chosen as
179 having the lowest percentage error under the last Rouquerol criterion. Further details on the BETSI
180 algorithm and the extension of the Rouquerol criteria can be found in **Section S3**, and a more
181 detailed description in **Section S14**. The source code is fully published under GitHub
182 <https://github.com/fairen-group/betsi-gui>.

183 **Figure 1** shows the comparison between BET areas calculated by researchers in the round-
184 robin evaluation and using BETSI. Bar a few exceptions, virtually no two groups of experts reported
185 identical BET areas for any given isotherm. The results are fully tabulated and graphically
186 represented in **Section S4** and **Section S5** respectively. We observed a spread of at least 300 m²
187 g⁻¹ for each isotherm; however, that number was significantly higher for some individual isotherms.
188 For NU-1104, a modern MOF with substantial porosity²² the highest estimate of 9,341 m² g⁻¹ and the
189 lowest estimate of 1,757 m² g⁻¹ differed by an astonishing 7,584 m² g⁻¹, making the highest estimate
190 more than five times higher than the lowest one. Most groups (90%) reported using the Rouquerol
191 criteria in their manual calculation, 23% used a commercial software package, and 6% used a self-
192 developed code. Full details on each individual group's methods can be found in **Section S13**.



193

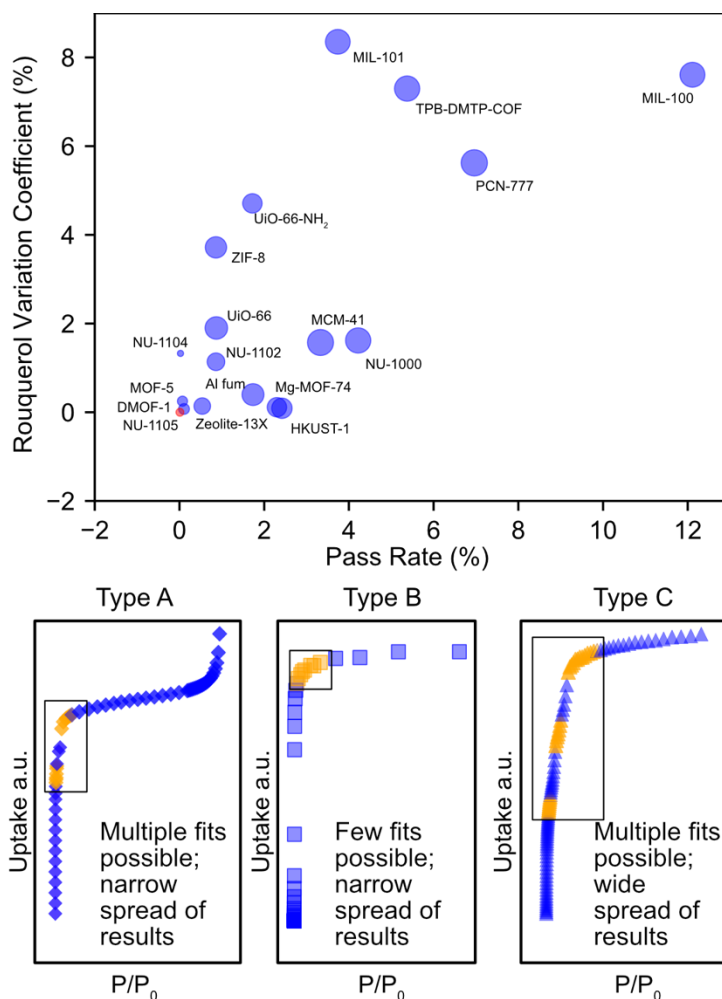
194 **Figure 1 | Round-robin results and BETSI results.** Distribution of BET areas from identical isotherms as
 195 calculated by 60 laboratories with expertise in adsorption science and synthesis of porous materials in red.
 196 Superimposed are normalised probability distribution functions obtained by kernel density estimation.
 197 Predictions under BETSI are shown in blue alongside, and the 'optimal' BET area in yellow.

198

199 Under BETSI, on the other hand, whilst multiple BET areas are passed as valid, the spread of
 200 values was considerably narrower than that obtained by manual calculation (**Figure 1**; for full BETSI
 201 results, see **Section S6** and further comparative data **Section S7**, **Section S8**, and **Section S9**).
 202 From this, both our first and second hypotheses are substantiated: since BETSI calculates *all* valid
 203 BET areas, it proves that the Rouquerol criteria by themselves are indeterminate and that even full
 204 compliance does not guarantee an unambiguous answer. Besides, since the spread of all valid BET
 205 areas is narrower than that obtained in the round-robin exercise, it demonstrates how the manual
 206 and systematic implementation of the Rouquerol criteria is difficult and often neglected in practice.
 207 For instance, in the case of NU-1104, the range of estimates decreases from 7,500 m² g⁻¹ in the
 208 social study to 235 m² g⁻¹ under BETSI.

209 Interestingly, some isotherms returned under BETSI much larger spreads of results than others,
 210 suggesting that they BET model does not describe them as naturally and thus they were more
 211 susceptible to problems associated with the Rouquerol criteria; a trend that was mirrored in the
 212 round-robin evaluation. To further investigate the goodness of the isotherm fittings, we define the
 213 *BETSI Variation Coefficient* as the relative standard deviation of BETSI results, and the *Pass Rate*
 214 as the number of BET fits that pass under the Rouquerol criteria as a fraction of all potential fits.

215 Further, the *Hit Rate* expresses the fractional number of BET areas calculated in the round-robin
216 exercise that lie within the BETSI range. **Figure 2** demonstrates the correlation between the *Pass*
217 *Rate*, the *BETSI Variation Coefficient*, and the *Hit Rate*. Simply put, the more BET fits are valid, the
218 greater the spread of possible BET areas is, and the more likely researchers are to satisfy the
219 Rouquerol criteria in manual calculations; an alternative representation can be found in **Section S10**.
220 From **Figure 2**, we classify adsorption isotherms into three broad categories, types A, B and C.
221 Whilst it is difficult to generalise about the shape of these isotherms, we offer some discussion about
222 common features in **Section S11**. Type A isotherms fit the BET model 'best'. Under BETSI, they
223 have a relatively high Pass Rate and return a fairly narrow spread of results. Examples include
224 materials such as Al fumarate, NU-1000, Zeolite-13X and MCM-41. Hit Rates greater than 70% are
225 generally observed for these materials, suggesting that the majority of researchers did not struggle
226 with the fittings. Type B isotherms only fit the BET model over a very limited range. These have
227 extremely low Pass Rates, meaning that only a few BET fits are valid, which in turn will be spread
228 narrowly. Examples include MOF-5, DMOF-1, NU-1104, HKUST-1, and NU-1105. For the latter, out
229 of 9,409 hypothetical 10-point fits (the minimum point requirement for BET fits), only one is
230 permissible under the Rouquerol criteria. Such prohibitively low Pass Rates make the correct BET
231 assignment by hand virtually impossible and demonstrate the need for computational support. Type
232 C isotherm fittings are arguably the most problematic. They have high Pass Rates and,
233 concomitantly, they return large spreads of BET results. Typical materials that fit into this category
234 are MIL-101, MIL-100, TPB-DMTP-COF and PCN-777. It is for these materials that the necessity to
235 extend the Rouquerol criteria is demonstrated and the BETSI algorithm makes an unambiguous BET
236 assignment possible.



237

238 **Figure 2 | Isotherm classifications.** Plot of the BETSI Variation Coefficient (relative standard deviation of
 239 BETSI results) against the Pass Rate (fraction of valid fits against all hypothetical ones). Bubble size scales
 240 with the Hit Rate, the fraction of results from the social study that lie within the BETSI range. Red symbols
 241 have a Hit Rate of zero. Note the positive correlation between all three parameters. Isotherm fit classifications.
 242 Type A fits have a relatively wide fitting window, within which multiple fits are possible, but return a relatively
 243 narrow spread of BET results. Type B fits have a narrow fitting window and concomitantly return a narrow set
 244 of spread of results. Type C fits have wide fitting windows, which translates to multiple passable fits and a wide
 245 spread of permissible BET areas.

246

247 In conclusion, BET theory is a great success story. Developed in the 1930s for open surfaces,
 248 it continues to be applied to modern adsorbents with complex porosities. Despite the advances from
 249 classical density functional theory (DFT) methods, the BET area will likely continue playing a crucial
 250 role in porosimetry for decades to come, with impacts in energy research, transport, medical
 251 applications and climate-change mitigation. In light of these future developments, it will become
 252 increasingly important to share critical scientific metrics reliably to find a common language to report
 253 both academic and industrial progress.

254 Here, we have demonstrated the difficulties in unambiguously determining BET areas from
 255 adsorption isotherms, which in turn affect the assessment of material quality and reproducibility.
 256 These problems arise from imperfect and insufficient manual calculations and can only be met using
 257 modern computational methods. BETSI is a step towards greater transparency and critical

258 assessment in reporting BET areas. We stress here that it is neither the function nor the purpose of
259 BETSI to eliminate doubt and treat a particular BET area as ‘true’. Researchers should remain aware
260 of the limitations of BET theory when applied to microporous adsorbents in general and when BET
261 areas are reported, the pressure range and number of points used should always be stated. We
262 further recommend here that isotherms must be reported transparently and in detail, *i.e.* semi-log
263 representation to show the low-pressure regions. The ‘experiment’ is the adsorption isotherm – not
264 the BET area.

265

266 **Online Content**

267 Any methods, additional references, source data, extended data, supplementary information,
268 acknowledgements, peer review information; details of author contributions and competing interests
269 are available at request.

270 Isotherm data reported with this paper are included in the NIST/ARPA-E Database of Novel and
271 Emerging Adsorbent Materials, <https://adsorption.nist.gov>, and may be accessed directly at
272 <https://adsorption.nist.gov/isodb/index.php?DOI=10.XXXX/YYYYY#biblio>.

273

274 **Bibliography**

- 275 1. Brunauer, S., Emmett, P. H. & Teller, E. Adsorption of Gases in Multimolecular Layers. *J.*
276 *Am. Chem. Soc.* **60**, 309–319 (1938).
- 277 2. Cid, R., Arriagada, R. & Orellana, F. Zeolites surface area calculation from nitrogen
278 adsorption data. *J. Catal.* **80**, 228–230 (1983).
- 279 3. Beck, J. S. *et al.* A New Family of Mesoporous Molecular Sieves Prepared with Liquid
280 Crystal Templates. *J. Am. Chem. Soc.* **114**, 10834–10843 (1992).
- 281 4. Kitagawa, S., Kitaura, R. & Noro, S. I. Functional porous coordination polymers. *Angew.*
282 *Chemie - Int. Ed.* **43**, 2334–2375 (2004).
- 283 5. Zhou, H. C., Long, J. R. & Yaghi, O. M. Introduction to metal-organic frameworks. *Chemical*
284 *Reviews* vol. 112 673–674 (2012).
- 285 6. Diercks, C. S. & Yaghi, O. M. The atom, the molecule, and the covalent organic framework.
286 *Science* **355**, (2017).
- 287 7. Li, J., Sculley, J. & Zhou, H. Metal-Organic Frameworks for Separations. *Chem. Rev.* **112**,
288 869–932 (2012).
- 289 8. Farha, O. K. *et al.* De novo synthesis of a metal-organic framework material featuring
290 ultrahigh surface area and gas storage capacities. *Nat. Chem.* **2**, 944–948 (2010).
- 291 9. Li, B., Wen, H.-M., Zhou, W. & Chen, B. Porous Metal–Organic Frameworks for Gas
292 Storage and Separation: What, How, and Why? *J. Phys. Chem. Lett.* **5**, 3468–3479 (2014).
- 293 10. Moghadam, P. Z. *et al.* Computer-aided discovery of a metal-organic framework with
294 superior oxygen uptake. *Nat. Commun.* **9**, 1378–1385 (2018).
- 295 11. Corma, A., García, H. & Llabrés i Xamena, F. X. Engineering Metal Organic Frameworks for
296 Heterogeneous Catalysis. *Chem. Rev.* **110**, 4606–4655 (2010).
- 297 12. Horcajada, P. *et al.* Metal-organic frameworks in biomedicine. *Chem. Rev.* **112**, 1232–1268
298 (2012).
- 299 13. Thommes, M. *et al.* Physisorption of gases, with special reference to the evaluation of

- 300 surface area and pore size distribution (IUPAC Technical Report). *Pure Appl. Chem.* **87**,
301 1051–1069 (2015).
- 302 14. Sing, K. S. W. *et al.* Reporting Physisorption Data for Gas/Solid Systems with Special
303 Reference to the Determination of Surface Area and Porosity. *Pure Appl. Chem.* **57**, 603–
304 619 (1985).
- 305 15. ISO [International Organization for Standardization]. Determination of the specific surface
306 area of solids by gas adsorption - BET method (ISO 9277:2010(E)). (2010)
307 doi:10.1007/s11367-011-0297-3.
- 308 16. Ambroz, F., Macdonald, T. J., Martis, V. & Parkin, I. P. Evaluation of the BET Theory for the
309 Characterization of Meso and Microporous MOFs. *Small Methods* **2**, 1800173 (2018).
- 310 17. Gómez-Gualdrón, D. A., Moghadam, P. Z., Hupp, J. T., Farha, O. K. & Snurr, R. Q.
311 Application of Consistency Criteria To Calculate BET Areas of Micro- And Mesoporous
312 Metal-Organic Frameworks. *J. Am. Chem. Soc.* **138**, 215–24 (2016).
- 313 18. Walton, K. S. & Snurr, R. Q. Applicability of the BET method for determining surface areas
314 of microporous metal-organic frameworks. *J. Am. Chem. Soc.* **129**, 8552–8556 (2007).
- 315 19. Park, J., Howe, J. D. & Sholl, D. S. How Reproducible Are Isotherm Measurements in Metal-
316 Organic Frameworks? *Chem. Mater.* **29**, 10487–10495 (2017).
- 317 20. Sinha, P. *et al.* Surface Area Determination of Porous Materials Using the Brunauer-
318 Emmett-Teller (BET) Method: Limitations and Improvements. *J. Phys. Chem. C* **123**, 20195–
319 20209 (2019).
- 320 21. Furukawa, H., Cordova, K. E., O’Keeffe, M. & Yaghi, O. M. The Chemistry and Applications
321 of Metal-Organic Frameworks. *Science* **341**, 1230444–1230444 (2013).
- 322 22. Wang, T. C. *et al.* Ultrahigh Surface Area Zirconium MOFs and Insights into the Applicability
323 of the BET Theory. *J. Am. Chem. Soc.* **137**, 3585–3591 (2015).
- 324 23. Fairen-Jimenez, D. *et al.* Opening the gate: Framework flexibility in ZIF-8 explored by
325 experiments and simulations. *J. Am. Chem. Soc.* **133**, 8900–8902 (2011).
- 326 24. Rouquerol, J., Llewellyn, P. & Rouquerol, F. Is the BET equation applicable to microporous
327 adsorbents? *Stud. Surf. Sci. Catal.* **160**, 49–56 (2007).
- 328 25. Rouquerol, J., Rouquerol, F., Llewellyn, P., Maurin, G. & Sing, K. S. W. *Adsorption by*
329 *Powders and Porous Solids: Principles, Methodology and Applications: Second Edition.*
330 *Adsorption by Powders and Porous Solids: Principles, Methodology and Applications:*
331 *Second Edition* (Academic Press, 2013). doi:10.1016/C2010-0-66232-8.
- 332 26. D.W. Siderius, V.K. Shen, R.D. Johnson III, and R.d. van Zee, Eds., NIST/ARPA-E
333 Database of Novel and Emerging Adsorbent Materials, National Institute of Standards and
334 Technology, Gaithersburg MD, 20899, <https://dx.doi.org/10.18434/T43882>, (retrieved Augu.
335 vol. 91).

336

337 **Acknowledgements**

338 This project has received funding from the European Research Council (ERC) under the European
339 Union’s Horizon 2020 research and innovation programme (NanoMOFdeli), ERC-2016-COG
340 726380. D.F.-J. thanks the Royal Society for funding through a University Research Fellowship.
341 Mark Carrington is acknowledged for his contribution to the COF isotherm.

342 O.K.F. and R.Q.S. acknowledge funding from the U.S. Department of Energy (DE-FG02-
343 08ER15967).

344 R.S.F. and D.B. acknowledge funding from the European Research Council (ERC) under the
345 European Union’s Horizon 2020 research and innovation programme (SCoTMOF), ERC-2015-StG
346 677289.

347 Sandia National Laboratories is a multimission laboratory managed and operated by National
348 Technology and Engineering Solutions of Sandia, LLC., a wholly owned subsidiary of Honeywell
349 International, Inc., for the U.S. Department of Energy's National Nuclear Security Administration
350 under contract DE-NA-0003525. The authors gratefully acknowledge funding from the U.S.
351 Department of Energy, Office of Energy Efficiency and Renewable Energy, Hydrogen and Fuel Cell
352 Technologies Office, through the Hydrogen Storage Materials Advanced Research Consortium
353 (HyMARC). This paper describes objective technical results and analysis. Any subjective views or
354 opinions that might be expressed in the paper do not necessarily represent the views of the U.S.
355 Department of Energy or the United States Government.

356 J.D.E acknowledges the support of the Alexander von Humboldt Foundation and the Center for
357 Information Services and High-Performance Computing (ZIH) at TU Dresden.

358 S.K.G. and S.M. acknowledge SERB (Project No. CRG/2019/000906), India for financial support.

359 K.K. and R.K. acknowledge Active Co. Research Grant for funding.

360 S.K. acknowledge funding from the European Research Council (ERC) under the European Union's
361 Horizon 2020 research and innovation programme (COSMOS), ERC-2017-StG 756489.

362 N.L. and J.G.M acknowledge funding from the European Commission through the H2020-MSCA-
363 RISE-2019 program (ZEOBIOCHEM – 872102) and the Spanish MICINN and AEI/FEDER
364 (RTI2018-099504-B-C21). N.L. thanks the University of Alicante for funding (UATALENTO17-05).

365 ICN2 is supported by the Severo Ochoa program from the Spanish MINECO (Grant No. SEV-2017-
366 0706)

367 S.M.J.R. and A.L wish to thank the Fund for Scientific Research Flanders (FWO), under grant nos.
368 12T3519N and 11D2220N. V.V.S. acknowledges the Research Board of the Ghent University and
369 funding from the European Union's Horizon 2020 research and innovation programme (consolidator
370 ERC grant agreement No. 647755 – DYNPOR (2015-2020)).

371 L.S. was supported by the EPSRC Cambridge NanoDTC EP/L015978/1

372 C.T.Y. and T.S.N. acknowledge funds from the National Research Foundation of Korea, NRF-
373 2017M3A7B4042140 and NRF-2017M3A7B4042235

374 P.F. and H. Y. acknowledge US Department of Energy, Office of Basic Energy Sciences, Materials
375 Sciences and Engineering Division under Award No. DE-SC0010596 (P.F.).

376 R.O would like to acknowledge funding support during his Ph.D study from Indonesian Endowment
377 Fund for Education-LPDP with the contract No. 202002220216006

378 S.W. and J.A. acknowledge funding from the Basque Government Industry Department under the
379 ELKARTEK and HAZITEK programs.

380 B.V.L, S.T.E and A.M.P acknowledge funding from the European Research Council (ERC) under
381 the European Union's Horizon 2020 Research and Innovation Program (Grant agreement no.

382 639233, COFLeaf), and the Deutsche Forschungsgemeinschaft (DFG) via the cluster of excellence
383 e-conversion (project number EXC2089/1-390776260).

384 VPT and JLR would like to acknowledge funding from the EPSRC (EP/R01650X/1).

385 M.A.v.d.V and D.R. are grateful for funding from the European Research Council (ERC) under the
386 European Union's Horizon 2020 research and innovation programme (grant agreement n° 759212)

387